

## Article

# Effect of Biochar on Soil and Water Loss on Sloping Farmland in the Black Soil Region of Northeast China during the Spring Thawing Period

Pengfei Yu <sup>1,2,3</sup>, Tianxiao Li <sup>1,2,3,\*</sup> , Qiang Fu <sup>1,2,3,\*</sup> , Dong Liu <sup>1,2,3</sup>, Renjie Hou <sup>1,2,3</sup> and Hang Zhao <sup>1,2,3</sup>

<sup>1</sup> School of Water Conservancy and Civil Engineering, Northeast Agricultural University, Harbin 150030, China; yupengfei9995@126.com (P.Y.); liudong9599@yeah.net (D.L.); hourenjie888@126.com (R.H.); m15663583512@163.com (H.Z.)

<sup>2</sup> Key Laboratory of Effective Utilization of Agricultural Water Resources of Ministry of Agriculture, Northeast Agricultural University, Harbin 150030, China

<sup>3</sup> Heilongjiang Provincial Key Laboratory of Water Resources and Water Conservancy Engineering in Cold Region, Northeast Agricultural University, Harbin 150030, China

\* Correspondence: litianxiao@neau.edu.cn (T.L.); fuqiang0629@126.com (Q.F.)

**Abstract:** Biochar, as a kind of soil amendment, has attracted wide attention from scholars in various countries, and the effects of biochar on soil and water loss have been well reported. However, soil erosion is significantly affected by geographical conditions, climate, and other factors, and research on the characteristics of soil erosion and the effects of biochar application in seasonally frozen soil areas is currently unclear. The purpose of this study was to explore the effect of corn straw biochar application on soil and water conservation during the spring thawing period. Specifically, through field experiments, the addition of 0, 6, and 12 kg m<sup>-2</sup> biochar on slopes of 1.8, 3.6, 5.4, and 7.2° and the effects on runoff and the soil erosion rate of farmland were analyzed. The results showed that in the 6 and 12 kg m<sup>-2</sup> biochar addition treatments, the saturated water content of the soil increased by 24.17 and 42.91%, and the field capacity increased by 32.44 and 51.30%, respectively. Compared with the untreated slope, with an increase in biochar application rate, runoff decreased slightly, and soil erosion decreased significantly. This study reveals that biochar can be used as a potential measure to prevent soil and water loss on sloping farmland in cold regions.

**Keywords:** evaluation of soil and water conservation; simulated rainfall events; soil denudation; water and sediment process



**Citation:** Yu, P.; Li, T.; Fu, Q.; Liu, D.; Hou, R.; Zhao, H. Effect of Biochar on Soil and Water Loss on Sloping Farmland in the Black Soil Region of Northeast China during the Spring Thawing Period. *Sustainability* **2021**, *13*, 1460. <https://doi.org/10.3390/su13031460>

Academic Editor: Danilo Spasiano

Received: 3 December 2020

Accepted: 25 January 2021

Published: 30 January 2021

**Publisher's Note:** MDPI stays neutral with regard to jurisdictional claims in published maps and institutional affiliations.



**Copyright:** © 2021 by the authors. Licensee MDPI, Basel, Switzerland. This article is an open access article distributed under the terms and conditions of the Creative Commons Attribution (CC BY) license (<https://creativecommons.org/licenses/by/4.0/>).

## 1. Introduction

Soil erosion has always been an environmental problem faced by humans. In modern times, the development of large-scale industry and agriculture has intensified the occurrence of soil erosion, causing sharp deterioration in the ecological environment, which severely restricts agricultural development and threatens the survival of humankind. There are many forms of soil erosion, and regional differences in climate characteristics, topography, and soil vegetation types result in different forms of soil erosion [1,2]. For example, the soil in the loess region of Northwest China tends to be loose, poorly agglomerated, and structurally unstable; thus, the soil can be susceptible to erosion due to rainfall and runoff [3]. However, in the black soil region of Northeast China, due to seasonal climate change, freeze–thaw cycling between winter and spring leads to soil accumulation in ditches caused by changes in soil structure, permeability, water conductivity, water content, strength, and aggregate water stability, which make the soil in this region vulnerable to erosion [4,5]. Soil erosion as a result of freezing and thawing is an important process and occurs mainly at high latitudes and high altitudes. When the environmental temperature changes, the water in the soil undergoes a phase change. This change results in the soil being mechanically damaged and then migrating and accumulating under the action of

gravity and runoff [6–8]. The soil erosion process caused by freezing and thawing is very complex; therefore, studying soil erosion under the action of freezing and thawing has important practical significance for regional agricultural development and environmental governance [9,10].

The black soil region in Northeast China is an important base of grain commodity production [11]. The black soil region is an area with a concentrated distribution of black soil, chernozem soil, and meadow soil. Because the surface of these soils is rich in organic matter (OM), they have an obvious black color and similar properties (The Ministry of Agriculture of the People's Republic of China, 1996) [12]. Therefore, the distribution areas of black soil, chernozem, and meadow soil are collectively referred to as the northeastern black soil region [13]. Most of the three large black soil areas in China are located in the northeast. Among them, the Songnen black soil area is the largest, at approximately 0.208 million km<sup>2</sup>, representing 65.38% of the agricultural land area in the northeast [14]. Due to the combined effects of agricultural development and seasonal changes, the soil and water losses in the region are significant. Yu et al. [15] showed that 37.9% of the cultivated land in this area was threatened by significant soil erosion. Therefore, mitigating soil erosion in this area is an urgent problem that must be solved.

In recent years, biochar has shown potential for retarding land degradation and enriching soil organic carbon (SOC), and it has received extensive attention from environmental departments in China and abroad [16,17]. Biochar is composed of a wide range of raw materials, including agricultural and forestry wastes, such as wood, straw, and fruit peels, as well as industrial and urban organic wastes [18]. The raw materials used for biochar production vary regionally [19–21]. For example, large areas of cotton are planted in the Yangtze River Basin of China [22]. In this area, cotton straw is used as the main raw material to produce biochar, while in Northeast China, where maize, rice, and soybean are the main crops, the straw remaining after harvesting provides sufficient raw material for the preparation of biochar. The total amount of agricultural waste produced in China in 2018 was  $9 \times 10^8$  tons. The safe disposal and utilization of carbon-rich biomass residues are major challenges [23]. Traditional methods (e.g., incineration) not only fail to effectively recycle resources but also lead to severe atmospheric pollution (emission of greenhouse gases).

The unique and large specific surface area and multiporous structure of biochar reduce soil bulk density, increase porosity, actively improve soil hydraulic parameters, and increase the soil water-holding capacity, thus aiding in overcoming land degradation and other issues [24,25]. Atkinson et al. [26] found that the incorporation of biochar into soil can affect soil physical properties, such as structure, texture, porosity, particle size distribution (PSD), and bulk density [27,28]. Biochar application can reduce soil bulk density and increase porosity, thus affecting soil infiltration, erosion, and runoff by affecting the soil hydraulic characteristics [21,29–32]. Biochar is an organic material obtained by pyrolysis and carbonization in the complete or partial absence of oxygen. Biochar has the characteristics of low density, a high pH value, a high cation exchange capacity (CEC), and high stability [33–35]. After biochar was applied to soil by Wang et al. [36], the proportion of carbon storage in the soil increased. In the application of biochar, Shang et al. [37] and Liu et al. [38] found that biochar increased the SOC content, supplemented mineral nutrients, reduced the use of agricultural chemical fertilizer, and increased crop yield. In the black soil area of Northeast China, Wei et al. [39] applied 50 t hm<sup>-2</sup> biochar to sloping farmland for two consecutive years; the generalized soil structure index (GSSI) was greatly improved, and water savings and yield increases were achieved. When biochar is mixed with soil, its porous structure reduces the soil bulk density [24], changes PSD [25], increases porosity [26], and actively improves soil hydraulic parameters and the soil water-holding capacity [29,30]. By affecting soil hydraulic characteristics, biochar application can affect soil runoff, infiltration, and erosion, thus helping to overcome land degradation [31,32].

Dong et al. [40] found that biochar is stable in dry–wet and freeze–thaw cycles and under tillage conditions in the field, and Kettunen and Saarnio [41] noted that biochar application can reduce nitrogen loss in winter soil and increase crop yield in the second

year. Zhou et al. [42], Lee et al. [43], and Sadeghi et al. [44] also found that the application of biochar to soil significantly reduced soil loss and increased inorganic nitrogen and total phosphorus contents to levels higher than those in untreated soil. However, previous studies have shown that the ability of biochar to improve soil quality, slope erosion, and soil physical and chemical properties depends on the type of soil and the amount of biochar applied [45]. In addition, the relationship between the effective amount of biochar on different slopes, the soil type, and other environmental factors remains unclear. For example, Li et al. [46] found that as the biochar application rate on a 27% slope on the Loess Plateau increased, the impact on soil and water loss increased. However, Peake et al. [47] determined that the lowest biochar content best enhanced soil water saturation, and Reddy et al. [48] believed that the water conductivity and shear strength of soils increased with a decrease in the applied biochar content. Therefore, among the different soil types and different slopes, the level to which biochar decreases soil erosion differs. Moreover, soil erosion is greatly affected by climate conditions, especially under the effects of dramatic climate change, and the occurrence of soil erosion may be aggravated [2]. Compared with nonfrozen soil areas, in seasonally frozen soil areas with high latitude and high altitude, the free–thaw process may be an important process leading to soil erosion [49]. When the environmental temperature changes rapidly, the water in the soil undergoes a phase transition, which leads to mechanical damage [50], and the resistance to erosion of the soil decreases [4].

A large number of studies have reported that biochar can reduce soil erosion; however, in seasonally frozen regions such as Northeast China, after freezing and thawing, it is not clear whether biochar has a positive effect on soil and water conservation during spring thawing. Moreover, research on soil erosion following freezing and thawing has been conducted mostly in indoor simulated freezing and thawing environments, while indoor simulated and natural environments have different climatic conditions; therefore, the impact of freeze–thaw action on soil erosion requires further study. Based on the freeze–thaw interactions in the cold northeastern region, outdoor sloped land on the Songnen Plain of Northeast China was selected as the research area of this study, and the impact of biochar on sloping farmland soil erosion was explored. The thawing period of the frozen spring soil layer was selected; an artificial rainfall simulation including runoff, infiltration, and soil erosion was conducted; and the effects of biochar content on the soil erosion of different slopes under these climatic conditions were explored.

## 2. Materials and Methods

### 2.1. Test Area Overview

The experiments were conducted at the comprehensive test site of the School of Water Conservancy and Civil Engineering at Northeast Agricultural University. The geographical location is 45°44′22″ N, 126°43′6″ E, and the average elevation is 138 m. The test area location is shown in Figure 1, and the experimental area is located in the southeastern part of the Songnen Plain of Northeast China [51]. The area is mainly dominated by plains and has a mid-temperate continental monsoon climate. The average daily temperature is between −2.66 and 7.92 °C, the four seasons are distinct, and rain is concentrated in the summer. The average annual precipitation is approximately 583 mm, and summer precipitation accounts for 65% of the total annual precipitation. The rainfall duration is short and concentrated between June and September. Winters are cold and prolonged, with a regional soil freezing period of approximately 110 days and a snowfall of approximately 109 mm from November to April [52].

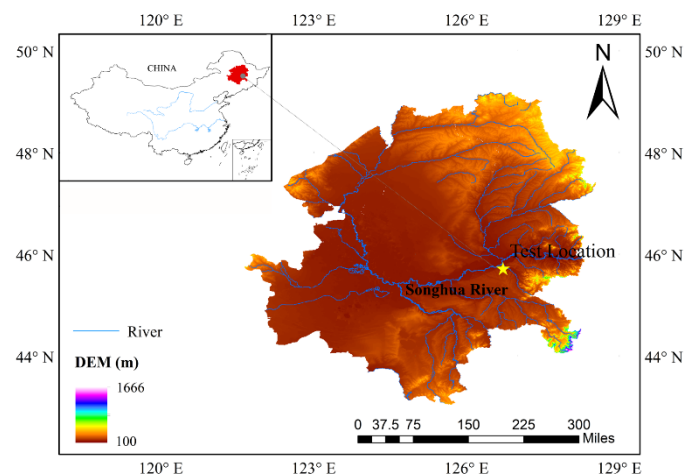


Figure 1. Test location.

Liu et al. [11] obtained slope information from  $90 \times 90$  m topographic survey (Shuttle Radar Topography Mission (SRTM)) data from the US space shuttle. The areas of land with slopes of  $0\text{--}1^\circ$ ,  $1\text{--}2^\circ$ ,  $2\text{--}3^\circ$ ,  $3\text{--}4^\circ$ ,  $4\text{--}5^\circ$ , and  $5\text{--}8^\circ$  accounted for 72.25, 17.77, 6.37, 2.12, 0.79, and 0.58% of the total area, respectively, and slopes of  $0\text{--}8$  degrees accounted for 99.88% of the total area. According to the USDA Soil Taxonomy, soil in the area is classified as Argiborolls, Haploborolls, Cryoborolls, and Haprostolls of mollisols, and the soil in this area is also listed as phaozem in the United Nations World Soil legend. In the Keys to Chinese Soil Taxonomy (3rd edition), the phaozem in Northeast China can be divided into three major types: black soil, chernozem, and meadow soil. The cultivated land vegetation is mainly corn and soybean and is grown in the drylands [53–55].

## 2.2. Test Methods

Rainfall was simulated using a rainfall simulation system with downward sprinkling. The artificial simulated rainfall equipment was designed and manufactured by Harbin Tianyu Automation Instrument Co., Ltd (Harbin, China). The rainfall simulator includes five nozzles, and the raindrop size and rainfall intensity can be adjusted by adjusting the nozzle aperture and water pressure, which can be set at any rainfall intensity between 50 and  $100 \text{ mm h}^{-1}$ . The rainfall height can be adjusted in the range of 2.5–3.5 m, the rainfall uniformity is greater than 85%, the simulated raindrop diameter distribution is approximately 0.15–3 mm, and approximately 80%–90% of the raindrop diameters are less than 1.5 mm. The above artificial rainfall parameters can evenly cover an area of  $2 \times 7$  m, which can meet the rainfall uniformity of each experimental plot; additionally, the size and distribution of simulated raindrops are similar to those of natural rainfall, and the simulated rainfall intensity was designed to be  $80 \text{ mm h}^{-1}$  given the intensity of erosion-causing rainstorms in the black soil area in Northeast China.

Twelve trapezoidal runoff test plots (5 m length, 2 m width) (No. P1–P12 in Table 1) with a slope adjusted from  $0$  to  $15^\circ$  by filling soil were used in this study. Each runoff test plot was trapezoidal box shape, the upper surface was of an inclined plane, and the lower surface was connected with the ground, as shown in Figure 2. The design gradients of this test were  $1.8^\circ$  (P1–P3),  $3.6^\circ$  (P4–P6),  $5.4^\circ$  (P7–P9), and  $7.2^\circ$  (P10–P12) because this slope range caused the most serious soil erosion in the northeastern black soil area during the last 30 years. The lower end of the test area was equipped with a collecting port, and runoff samples were collected through the connected bucket. The soil used was collected from the plow layer in Harbin, located in the black soil area of Northeast China. The soil in the experimental plot was loaded according to the soil type of the sloped farmland in the black soil area. Impurities such as gravel and straw were removed from the soil. To best retain its natural state, the soil was not sifted; thus, its aggregates maintained their original aggregation state and manually filled into the test plots. After adding the parent material

layer soil, the soil was compacted artificially, then the surface layer soil was added, and the same autumn plowing treatment as the local farmland was used. The surface layer of 0–30 cm was classified as loam (particle size fractionation: 46.3% sand, 20.4% silt, and 33.3% clay), and the bulk density was approximately  $1.15 \text{ g cm}^{-3}$ . The 30–60 cm parent material was clay loam, and the particle size fractionation was 38.7% sand, 24.7% silt, and 36.6% clay. The average bulk density of the soil was  $1.30 \text{ g cm}^{-3}$ , which is the same as that of the bottom of the plow layer in the northeastern black soil area.

**Table 1.** Slope gradient and biochar application in the experimental plots.

Biochar Content ( $\text{kg m}^{-2}$ )	Slope ( $^{\circ}$ )			
	1.8	3.6	5.4	7.2
0	P1	P4	P7	P10
6	P2	P5	P8	P11
12	P3	P6	P9	P12

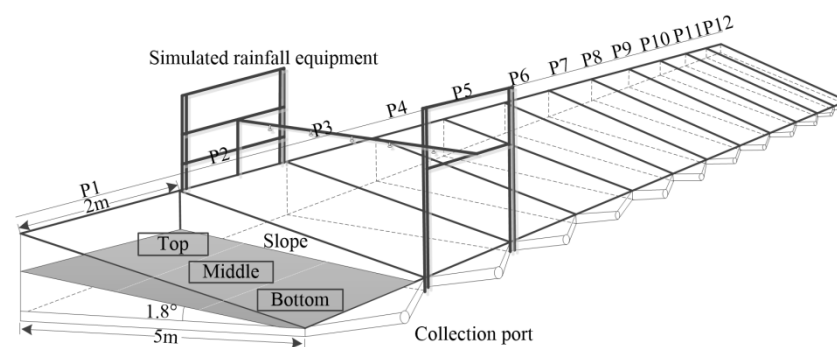


**Figure 2.** Sketch of the test areas.

The biochar used was corn straw biochar purchased from Liaoning Jinhefu Agricultural Development Co., LTD (Anshan, China). The preparation of this biochar involves high-temperature cracking at 450 to 500  $^{\circ}\text{C}$  under low-oxygen or limited-oxygen conditions. The basic physical and chemical properties are as follows: particle size of 1.5–2.0 mm, pH value of 9.14; nitrogen content of 1.53%, phosphorus content of 0.78%, potassium content of 1.68%, total organic carbon (TOC) content of  $409.7 \text{ g kg}^{-1}$ , and ash content of 31.8%.

From late September to early October 2017, 0, 6, and  $12 \text{ kg m}^{-2}$  biochar was applied on the surface of the test area at a depth of 0–30 cm. The biochar was evenly mixed with the cultivated soil by the traditional agricultural tillage method, and a biochar–soil mixed layer (approximately 0–30 cm) was formed. The control group ( $0 \text{ kg m}^{-2}$ ) was also tilled to the same extent. The volume ratio of biochar to 0–30 cm surface layer soil was approximately 3.33–6.67%. Table 1 shows the amount of biochar applied in each test area.

During the freeze–thaw period from October to April of the next year, plots P1–P12 in the test area were allowed to keep their natural snow cover without human interference. The test areas were adjacent to each other, with no differences in climate or environment. On 8 April 2018, 9 equidistant sampling points ( $3 \times 3$ ) were selected for each plot. Undisturbed soil samples (0–10 cm) were collected by the cutting ring method [56], the natural water content was determined by the drying method [57], the content of soil organic matter was determined by the potassium dichromate oxidation external heating method [58], and a simulated rainfall experiment was carried out. The meteorological conditions on that day were as follows: the average daily temperature was  $0.3 \text{ }^{\circ}\text{C}$ , the average wind speed was  $2.6 \text{ m s}^{-1}$ , the average relative humidity was 56%, the daily evaporation rate was  $2.8 \text{ mm d}^{-1}$ , the accumulated precipitation was 0.2 mm, and there was no precipitation in the test area on that day. The meteorological data were collected from the China Meteorological Data Network (<http://data.cma.cn/>). On 8 April, the range of the thawing depth was 45–50 cm, and the frozen soil depth was measured by using a frozen soil device

composed of a PVC pipe and rubber hose (LQX-DT, Jinzhou Licheng, Jinzhou, Liaoning, China) [51]. To ensure that the initial water content of each plot was consistent and to minimize the impact of rainfall on the thawing depth, a rainfall pretreatment with a rainfall intensity of  $80 \text{ mm h}^{-1}$  was carried out 24 h before the test. When runoff appeared on the slope, the rainfall was stopped immediately to ensure that the initial soil moisture content of all slopes reached saturation. In the rainfall-runoff experiment, the time started when runoff appeared on the slope and lasted for 40 min. Three repeated rainfall experiments were carried out in each plot. The runoff water and eroded soil material were collected through the collection port of the test chamber [59], and the time was recorded with a timer with an accuracy of 0.01 s [60]. The runoff water and eroded soil material were collected every 5 min after runoff generation, and the method of sample collection was consistent throughout the test. After the rainfall, all samples were weighed with an electronic balance with an accuracy of 0.01 g, and the runoff was measured. Then, the samples were allowed to stand for 12 h for sedimentation. After removing the supernatant, the sediment mixtures were put into an oven, dried at  $105 \text{ }^\circ\text{C}$  for more than 24 h, and then weighed with an electronic balance with an accuracy of 0.01 g [61].

### 2.3. Calculation of the Average Infiltration Rate

Water infiltration into the soil is a dynamic process in which water, such as water from rainfall and runoff, migrates under the action of gravity and other potential forces and is stored as soil water. The extent of bare soil and the soil texture and slope under the same rainfall and intensity conditions are important factors affecting the amount of soil infiltration. The soil infiltration rate is an important index reflecting soil permeability characteristics because it directly reflects the soil water retention capacity. According to rainfall and runoff data, the average infiltration rate of a slope under the conditions of unchanged rainfall and rainfall intensity can be calculated according to Formula (1) [62]:

$$f_i = \frac{Pt \cos \alpha - \frac{10R}{S}}{t} \quad (1)$$

where  $f_i$  represents the average infiltration rate of the slope ( $\text{mm min}^{-1}$ ),  $P$  represents the rainfall intensity ( $\text{mm min}^{-1}$ ),  $\alpha$  represents the slope ( $^\circ$ ),  $t$  represents the rainfall time (min),  $R$  represents the runoff (mL) generated during rainfall time  $t$ , and  $S$  represents the actual rain-affected area ( $\text{cm}^2$ ).

### 2.4. Grey Relational Projection Model

The main factors affecting soil and water conservation were determined. In this study, the soil water-holding capacity, runoff, and soil loss rate were selected as indicators for the grey relational projection method. The test results were made dimensionless by the extremum method [63]. Generally, the indexes of the grey relational projection model include "benefit type" and "cost type." The benefit index refers to the index with the larger attribute value, the better; the cost index refers to the index with the smaller attribute value, the better. The effect of soil and water conservation includes soil water-holding capacity, runoff rate, infiltration rate, and soil loss rate. These indexes have "benefit type" and "cost type" indexes, respectively. Therefore, 12 runoff plots are regarded as 12 soil and water conservation schemes, and the grey relational projection model is used to find the relative best decision-making scheme among the 12 schemes. In the grey relational projection model, it is necessary to determine the weighted vector of the index. The analytic hierarchy process (AHP) can decompose the relevant key index factors according to the actual problems. By constructing the judgment matrix, the weight of the key factors can be calculated through the matrix. After the consistency test, it provides an objective and scientific judgment method for comprehensive decision-making. The judgment matrix  $A = (a_{ij})_{n \times n}$  is constructed by using the numbers 1–9 and their reciprocals as the scales of each criterion layer and index layer. The judgment matrix, ranking calculation, and consistency test together formulate a persuasive final result that has obvious advantages

compared with other methods, making this approach more suitable for determining the weight of the evaluation index of a decision scheme. Test plots P1 to P12 were considered to correspond to 12 schemes, and the grey correlation projection value of each scheme was calculated.

The decision matrix is determined as follows. The set of runoff and soil conservation schemes in the 12 small areas is defined as A. The soil and water conservation index set of the experimental plot is V. The value matrix  $Y_{ij}$  of scheme  $A_i$  is attributed to evaluation index  $V_j$ :

$$A = \{P1, P2, \dots, P12\} \quad (2)$$

$$V = \{\text{moisture content, infiltration rate, soil loss rate}\} \quad (3)$$

$$Y_{ij}(i = 1, 2, \dots, 12; j = 1, 2, 3) \quad (4)$$

The optimal scheme of the three indexes is selected, comprising the maximum moisture content, the maximum infiltration rate, and the soil loss rate from the test data. The optimal residual augmented matrix is formed with the original indicators.

$$Y = [Y_{ij}]_{(12+1) \times 3} (i = 0, 1, 2, \dots, 12; j = 1, 2, 3) \quad (5)$$

The evaluation index is dimensionless, and the initial decision matrix  $Y'_{ij}$  is obtained.

$$Y'_{ij} = Y_{ij}/Y'_{0j}, i = 0, 1, 2, \dots, 12; j = 1, 2, \dots, 3. \quad (6)$$

The grey correlation matrix  $r_{ij}$  is determined, and the coefficient  $\gamma$  is taken as 0.5.

$$r_{ij} = \frac{\min_{12} \min_3 |Y'_{0j} - Y'_{ij}| + \gamma \max_{12} \max_3 |Y'_{0j} - Y'_{ij}|}{|Y'_{0j} - Y'_{ij}| - \gamma \max_{12} \max_3 |Y'_{0j} - Y'_{ij}|} \quad (7)$$

The grey relational judgment matrix  $f$  composed of  $r_{ij}$  is established.

$$F_{ij} = \begin{pmatrix} F_{01} & F_{02} & F_{03} \\ F_{11} & F_{12} & F_{13} \\ \vdots & \vdots & \vdots \\ F_{12\ 1} & F_{12\ 2} & F_{12\ 3} \end{pmatrix} \quad (8)$$

If the evaluation index of weighted vector  $W = [W_1, W_2, W_3]^T > 0$ , the weight is normalized, and  $\bar{W}_j$  is the grey correlation projection weight vector.

$$\bar{W}_j = W_j^2 / \sqrt{\sum_{j=1}^m W_j^2}, j = 1, 2, 3. \quad (9)$$

On the basis of Formulas (8) and (9), the grey correlation projection value  $D_j$  is calculated.

$$D_j = F_{ij} \bar{W}_j, j = 1, 2, 3. \quad (10)$$

The larger the projection value  $D_j$  of a given test scheme is, the closer the test results are to the optimal result.

## 2.5. Analytical Methods

SPSS 22 and Origin 2017 were used for data processing, drawing, and tabulating. Data points were summarized by calculating the mean and standard deviation. The least-significant difference (LSD) method of single-factor square analysis (ANOVA) was used to test the difference in slope water content and sediment loss in different treatment modes with a significance level of  $p = 0.05$ .

### 3. Results

#### 3.1. Effects of Biochar on the Natural Moisture Content of the Slope Surface

The basic slope soil physical indicators after biochar application are shown in Table 2. The saturated water content and field water-holding capacity of the soil were significantly higher than those of the soil without biochar application and increased as the amount of biochar applied increased. However, after the first application of biochar and freezing in winter, during the thawing period in spring, the soil OM content changed slightly.

**Table 2.** Basic soil physical properties after biochar application.

Biochar Application Rate (kg m <sup>-2</sup> )	Saturated Moisture Content (g kg <sup>-1</sup> )	Field Water-Holding Rate (g kg <sup>-1</sup> )	Dry Weight of Soil (g cm <sup>-3</sup> )	Organic Matter (OM) Content (g kg <sup>-1</sup> )
0	392.7 ± 9.73	281.7 ± 3.15	1.43 ± 0.015	38.6 ± 0.95
6	487.6 ± 8.58	373.1 ± 6.26	1.35 ± 0.018	39.1 ± 1.36
12	561.2 ± 7.21	426.2 ± 3.86	1.17 ± 0.013	38.8 ± 0.89

Note: The results are presented as the means ± standard deviations ( $n = 3$ ), and the data in the table were measured before the simulated rainfall.

As shown in Figure 3, compared with those of the untreated plot (P1), the natural moisture contents of P2 and P3 were significantly higher at a slope of 1.8° ( $p < 0.05$ ), and the difference between P2 and P3 was not significant. This result indicated that biochar played a role in increasing the natural water content on this slope, but the difference between 6 and 12 kg m<sup>-2</sup> was not significant. The natural water content of P6 was significantly higher than that of P4 at a 3.6° slope ( $p < 0.05$ ). The difference in the natural water content of P5 from those of P4 and P6 was not significant, indicating that only biochar application at 12 kg m<sup>-2</sup> played a significant role in increasing the natural water content of soil at a 3.6° slope. There was no significant difference in natural water content between the biochar-treated slopes at 5.4° (P7–P9) and 7.2° (P10–P12) and the untreated slopes. The results showed that the natural water content of the slope at 1.8° significantly increased with biochar application. Only biochar application at 12 kg m<sup>-2</sup> on the 3.6° slope significantly increased the natural water content. It may be that the gradients of 5.4 and 7.2° were relatively large. Under the action of gravity, the adsorption of water by the medium and large voids after applying biochar was insufficient, which led to the movement of water to the bottom of the slope and the failure to improve the water-holding capacity of the soil.

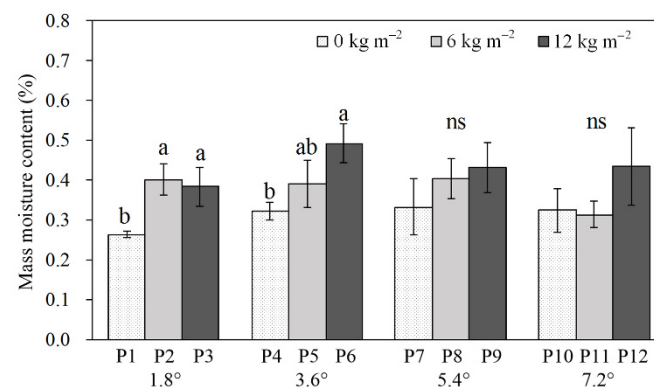


**Figure 3.** Mass soil moisture content of each of the twelve experimental plots before the simulated rainfall. Error bars represent the standard deviations of means ( $n = 3$ ). In each gradient, the different letters (a, b) indicate significant differences between treatments at the  $p < 0.05$  level according to the least-significant difference (LSD) test; ns denotes nonsignificant.

#### 3.2. Effects of Biochar on Rainfall Runoff and Slope Infiltration during the Thawing Period

The runoff and infiltration rates of the slopes are shown in Figure 4. According to the change in runoff rate, 0–40 min was divided into a nonsteady stage from 0 to 20 min

and a quasisteady stage from 20 to 40 min. The runoff and infiltration on the slope were analyzed. Overall, in the  $1.8^\circ$  slope test plot, the runoff rate began to increase rapidly in the nonsteady stage, and the difference between the three treatments was small and gradually stabilized in the quasisteady stage. In the quasisteady stage, the runoff rate was ranked  $P1 > P2 > P3$  and decreased with increasing biochar content. The infiltration rate decreased rapidly in the nonsteady stage. In the quasisteady stage, the average infiltration rate of the plots treated with 6 and  $12 \text{ kg m}^{-2}$  biochar increased by 3.94% and 7.12%, respectively. In the  $3.6^\circ$  test plots, the runoff rates of P4, P5, and P6 were almost the same in the nonsteady stage. In the quasisteady stage, the runoff rate of P4 continued to increase, exceeded the runoff rates of P5 and P6, and tended to become stable; the average infiltration rates of the P5 and P6 plots increased by 6.68% and 11.44%, respectively. Although the runoff rates of P8 and P9 were less than that of P7 among the  $5.4^\circ$  test plots, biochar application had little effect on the runoff rate at this slope.

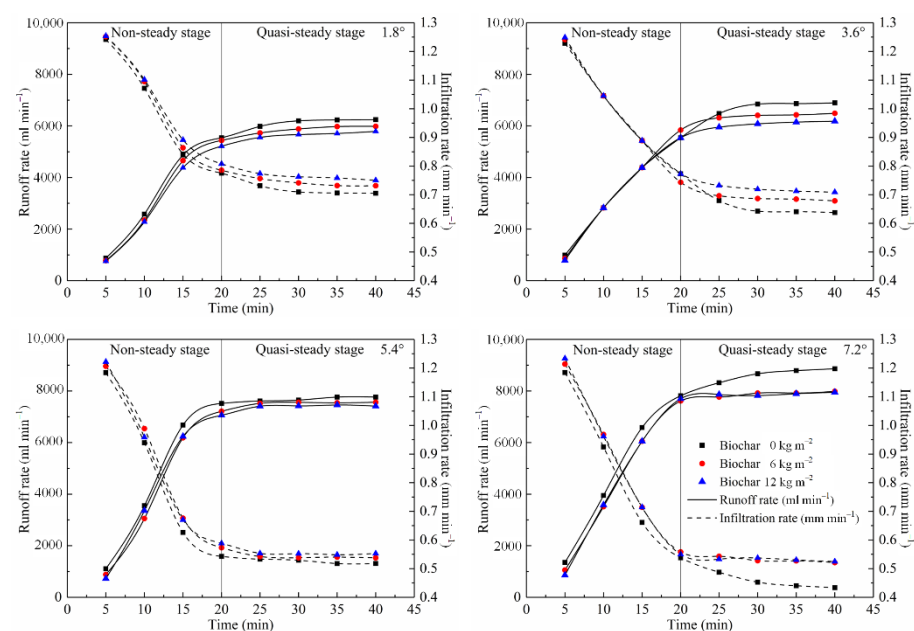


**Figure 4.** Runoff and infiltration rates of the four slopes from 0 to 40 min.

In the quasisteady stage, the average infiltration rates of P8 and P9 increased by 3.42% and 5.58%, respectively, compared with that of P7. In the  $7.2^\circ$  test plots, the runoff rates of P11 and P12 decreased significantly compared with that of P10, and the difference between P11 and P12 was very small. The runoff rates under biochar application at 6 and  $12 \text{ kg m}^{-2}$  decreased with the slope. However, the difference between the two biochar treatments was very small. Compared with that of P10, the average permeation rates of P11 and P12 in the quasisteady stage increased by 16.97% and 17.38%, respectively.

### 3.3. Effects of Biochar on the Soil Loss Rate of the Slopes

The soil loss rate ( $\text{g m}^{-2} \text{ min}^{-1}$ ) is the mass of sediment lost per unit time and unit area of soil on a slope under the interaction of rainfall and runoff [64]. The variation in the soil loss rate with rainfall duration on the four slopes is shown in Figure 5.

Within 0–20 min after the onset of runoff, the soil loss rates of plots P1–P12 rapidly increased; the soil loss rates tended to become stable from 20 to 40 min. We also found that in the quasistable stage, the effects of slope and biochar content on the soil loss rate were significant ( $p < 0.001$ ), as shown in Table 3.

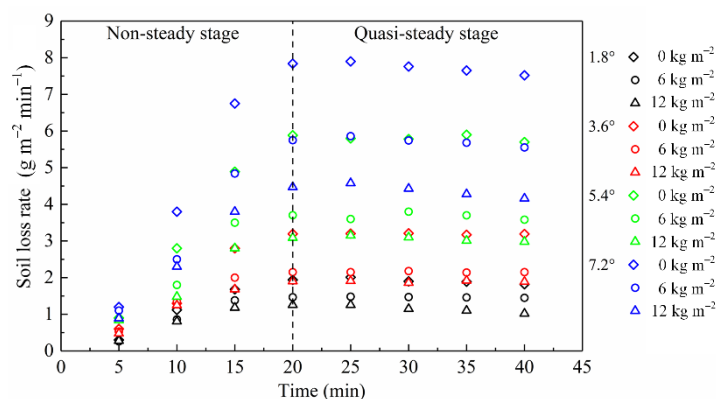


Figure 5. Soil loss rate of the four slopes from 0 to 40 min under the three treatment conditions.

Table 3. Average soil loss rate (g m<sup>-2</sup> min<sup>-1</sup>) of the four slopes under the three treatment conditions in the quasistable stage from 20 to 40 min. n = 4. Values of the soil loss rate followed by different letters (i.e., a through c and A through D) are significantly different at p < 0.001 according to ANOVA. Different capital letters in the same row indicate significant differences on different slopes with the same biochar content (p < 0.001); different lowercase letters in the same column indicate significant differences in biochar content on the same slope (p < 0.001).

Biochar Content (kg m <sup>-2</sup> )	Slope Gradient (°)			
	1.8°	3.6°	5.4°	7.2°
0	1.905 ± 0.068 Da	3.193 ± 0.015 Ca	5.795 ± 0.071 Ba	7.708 ± 0.140 Aa
6	1.465 ± 0.011 Db	2.155 ± 0.015 Cb	3.670 ± 0.088 Bb	5.708 ± 0.112 Ab
12	1.132 ± 0.086 Dc	1.895 ± 0.023 Cc	3.060 ± 0.068 Bc	4.363 ± 0.158 Ac

In the quasistable stage, the soil loss rates under biochar application at different concentrations were significantly different at the same slope (p < 0.001), the soil loss rates were significantly lower than those under no treatment at the same slope, and the soil loss rates under 12 kg m<sup>-2</sup> biochar application were less than those under no treatment or 6 kg m<sup>-2</sup> biochar application. Under the same treatment conditions, the soil loss rate significantly differed among slopes (p < 0.001). Under the same biochar application rate, the soil loss rate increased with increasing slope.

In the total runoff period from 0 to 40 min, compared with those of P1, the soil loss rates of P2 and P3 decreased by 21.37% and 32.75%, respectively; at 3.6°, the soil loss rates of P5 and P6 were 24.88% and 33.35% lower than that of P4, respectively; and at 7.2°, the soil loss rates of P8 and P9 were 31.54% and 41.61% lower than that of P7, and those of P11 and P12 were 25.16% and 40.71% lower than that of P10. According to the above results, the effect of 6 and 12 kg m<sup>-2</sup> biochar application on reducing the soil loss rate first increased and then decreased with increasing slope gradient. Under these conditions, the rate of soil loss decreased the most at 5.4°, by 31.54% and 41.61% for 6 and 12 kg m<sup>-2</sup> biochar applications, respectively. Although there were differences among previous studies in terms of the amount of biochar applied, soil type, and climatic conditions, similar results in the literature show that biochar has a significant effect on reducing soil loss on slopes.

### 3.4. Evaluation of the Soil and Water Conservation Ability of Test Plots P1–P12 Based on the Grey Relational Projection Model

The weighted values of the three characteristic indexes correspond to eigenvector values of 0.086, 0.258, and 0.657. The projection values (D<sub>j</sub>) of test plots P1–P12 obtained through the grey relational projection model are shown in Figure 6. The D<sub>j</sub> of P3 was larger than that of P2. The D<sub>j</sub> of P2 was larger than that of P1. The D<sub>j</sub> under 12 kg m<sup>-2</sup> biochar application was higher than that under 6 kg m<sup>-2</sup> biochar application for the same slope. This result was also found in the test plots with slopes of 3.6, 5.4, and 7.2°. The

$D_j$  of the biochar-treated test plots was higher than that of the plot with no biochar at the same slope, and the  $D_j$  of the test plot under  $12 \text{ kg m}^{-2}$  biochar application was higher than that of the test plot under  $6 \text{ kg m}^{-2}$  biochar application. In other words, biochar can enhance soil and water conservation on the slope of  $1.8\text{--}7.2$  degrees, and the effect of B12 treatment was the most significant. In addition, the  $D_j$  values under  $12 \text{ kg m}^{-2}$  biochar application at  $3.6$ ,  $5.4$ , and  $7.2^\circ$  were higher than those under no treatment at  $1.8$ ,  $3.6$ , and  $5.4^\circ$ . The results show that biochar application can effectively control soil and water losses on sloping farmland with gradients between  $1.8$  and  $7.2^\circ$  after freezing and thawing and that the effect of the biochar application rate on soil and water conservation is consistent in this gradient range. In the test plots with slopes between  $1.8$  and  $7.2^\circ$ , the degree of soil and water loss after biochar application was less than that in the untreated test plot, but the loss in the untreated plot was lower at  $1.8^\circ$ .

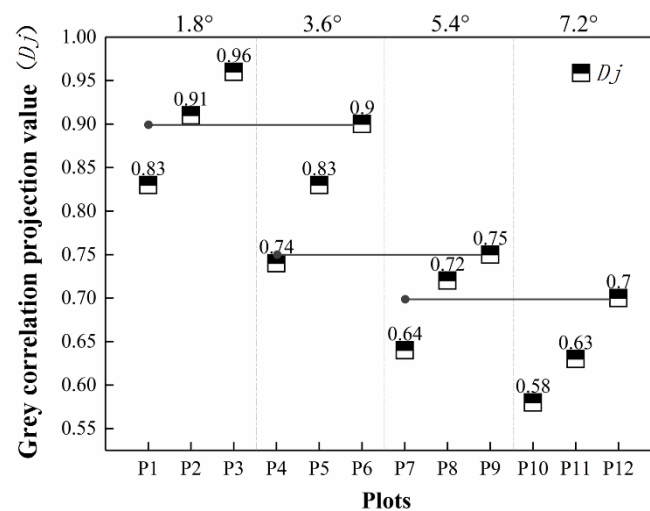


**Figure 6.** Grey relational projection model results for P1–P12. The function of the horizontal line in the figure is only for a more intuitive horizontal comparison.

#### 4. Discussion

Usually, the water storage capacity of soil after biochar application increases with the number of medium and large aggregates and the soil pore size ( $30\text{--}75 \mu\text{m}$ ) [65], and the pores in biochar itself can also store water. Fu et al. [65] considered that the effect of the combined application of biochar and freeze–thaw cycling on soil water content was mainly achieved by reducing the proportion of micropores ( $<0.3 \mu\text{m}$ ) in the soil layer and increasing the proportion of medium pores ( $>30\text{--}75 \mu\text{m}$ ). Therefore, under the same natural conditions, the natural water content of the soil treated with biochar was higher than that of the untreated soil, and the soil water content at  $1.8$  and  $3.6^\circ$  was significantly affected by biochar application. However, the two biochar treatments at  $5.4$  and  $7.2^\circ$  had less of an effect on the soil water content. The soil dry weight decreased as the amount of applied biochar increased, which is consistent with the effect of biochar on basic soil physical properties reported by Li et al. [66]. The soil moisture content in the spring during the thawing period is higher than that of dry unfrozen soil, which is affected by the melting snow water [67]. Brodowski et al. [68], and Sachdeva et al. [69] believed that the main mechanism of the bioenhancement of soil OM was that biochar particles are the core component and are gradually covered by clay, silt, and OM particles. The reason for the small change in the soil OM content may be because biochar application occurs in autumn, and the subsequent lower ambient temperature and the freezing effect of winter cause the biochar to freeze for most of the winter, but measurements were taken in the thawing period of the freezing and thawing process. As a result, the OM and microorganism contents in the biochar and soil particles were not fully aggregated in the following spring, and because the microorganisms in the soil had a low activity for a long time, the rate of

decomposition of animal and plant residues was slow [70], resulting in a very small change in OM content.

The slope runoff rate is an important factor affecting soil erosion [46]. He et al. [71] found that when biochar was mixed with soil, the soil intergranular pore space could increase through the presence of macrovoids in the biochar, thus improving the efficiency of soil water movement, increasing the soil permeability rate, and reducing the runoff rate. Liu et al. [72] reported that biochar is an important factor in changing soil properties. Similar to the results of Jien and Wang [45], Lee et al. [73] and Sadeghi et al. [32], appropriate biochar application was used to protect the soil surface from scabbing and increase the seepage rate, thus delaying the runoff generation time and reducing runoff. In this study, the difference between the two biochar treatments was less than 1%. The results show that biochar can increase the infiltration rate and reduce rainfall runoff on slopes, which is similar to the results of Sadeghi et al. [32]. Smetanova et al. [74] showed that 10% biochar application could increase the soil infiltration rate, reduce runoff events by up to 40%, and decrease the runoff coefficient by 16%. Bissonnais et al. [75] also found that biochar could reduce the impact of runoff on slopes and enhance the resistance of soil to raindrop impacts and runoff scouring. In this study, the runoff rate of the biochar-treated plots was slightly lower than that of the untreated plots at the same slope, but the differences were less than those in previous studies due to the limited conditions of the test site, climatic conditions, and other factors. To ensure a consistent freezing depth, the test utilized limited climatic and geographical conditions. The effect of biochar on the infiltration rate in this study may be related to the thawing depth. Therefore, it can be considered that the influence of biochar on slope runoff is constrained by the amount of biochar applied, the soil type, and the slope. Similar to the results of this experiment, a previous study found that the effect of biochar application on slope runoff was not significant in the red soil sloping farmland of southern China [76]. In contrast, the results of Jien and Wang [45] and Abrol [77] showed that with an increase in the amount of biochar applied, the control effect on slope runoff decreased. We speculate that perhaps there were differences in slope and soil texture.

Raindrops detach soil particles, destroy soil structure, and finally increase runoff and soil erosion [61]. Lee et al. [78] speculated that biochar could stabilize soil aggregates and form loose biochar–soil mixtures under Coulomb and van der Waals forces; these mixtures could absorb or buffer the energy of larger raindrops to prevent the separation of soil particles and soil scabs, thus reducing soil loss. Abrol et al. [77] significantly reduced soil loss by biochar application. These authors believed that biochar increased the soil surface roughness and that a large number of biochar particles accumulated on the soil surface. Greater soil surface roughness will likely interfere with the lateral movement of separated soil particles in runoff, thus reducing soil transport. Jien and Wang [45] and Doan et al. [79] found that the application of biochar could reduce the soil loss rate by 15–78%. In our study, soil loss decreased by 21.37–41.61%, similar to the soil loss reduction reported by Li et al. [46], and biochar application had an obvious effect on reducing soil erosion. In addition, we found some black biochar particles during the collection of runoff. We speculate that biochar may migrate upward because higher-density sand particles displace lower-density biochar particles and that the influence of raindrops helps this migration. We consider another dynamic mechanism of biochar migration to the upper soil layer to be buoyancy because of the tar and oil on the biochar surface, as biochar itself is hydrophobic and its dry density is lower than that of water [80]. It may also be that the very fine fraction of biochar particles move upward toward the biochar near the surface and that water can penetrate and fill most of the voids in the soil particles. New pore spaces in shallow soils are available for deep biochar entry. Some studies have also found biochar particles in runoff [32], which means that biochar application may need to be combined with treatment measures such as straw mulching, fertilizer application, or polyacrylamide treatment to improve the viscosity of biochar and soil particles and avoid floating after rainfall.

The soil and water conservation effects of the 6 and 12 kg m<sup>-2</sup> biochar treatments significantly improved in the spring thawing period after the winter freezing period, and the effect of the 12 kg m<sup>-2</sup> biochar treatment was higher than that of the 6 kg m<sup>-2</sup> biochar treatment. This finding is similar to the results of many scientific studies on the influence of biochar on slope runoff [17,66]. However, the conditions in Abrol et al. [77] and Wei et al. [80] did not include freeze–thaw effects after biochar treatment, as a result of which biochar had a lower effect on the slope runoff rate but a similar effect on significantly reducing the soil loss rate. The soil and water conservation effects of the 6 kg m<sup>-2</sup> and 12 kg m<sup>-2</sup> biochar treatments were evaluated by the grey relational projection method. The results showed that biochar treatment could improve the degree of soil and water conservation, and the effect of the 12 kg m<sup>-2</sup> biochar treatment was higher than that of the 6 kg m<sup>-2</sup> biochar treatment in the range of 1.8° to 7.2°. Therefore, biochar treatment can be used as a soil conditioner to improve soil and water conservation in seasonally frozen soil areas. To further improve the economic efficiency of biochar application, exploring the most appropriate biochar dosage in different slope ranges should be the focus of research related to the large-scale application of biochar.

## 5. Conclusions

Three different proportions of corn straw biochar were used on four different slopes in a seasonally frozen soil area. The results showed that biochar had a positive effect on the soil water-holding capacity of the 0–20 cm soil layer on plots with small slopes, which was beneficial for improving the soil and water conservation effects. However, when the slope increased, the effect of biochar treatment on the soil water-holding capacity was limited. In addition, the soil loss rates of the 6 kg m<sup>-2</sup> and 12 kg m<sup>-2</sup> biochar treatments decreased significantly in the spring thawing period and increased with increasing biochar content. The grey correlation results for the effects of biochar on slope soil and water conservation showed that the effects of the two biochar treatments on soil and water conservation were better than those of no treatment. The results of the field experiment with seasonal freezing and thawing show that biochar treatment has a positive effect on reducing the soil loss rate in seasonally frozen soil areas. For the extensive application of biochar, we also need to understand the matching of different biochar types and amounts with different soil types in long-term experiments, and the impact on soil organic matter is also worth further exploration.

**Author Contributions:** Conceptualization, Q.F. and T.L.; methodology, D.L.; software, Q.F.; validation, Q.F., T.L. and D.L.; formal analysis, R.H.; investigation, H.Z.; resources, Q.F.; data curation, T.L.; writing—original draft preparation, P.Y.; writing—review and editing, P.Y.; visualization, H.Z.; supervision, T.L.; project administration, R.H.; funding acquisition, Q.F. All authors have read and agreed to the published version of the manuscript.

**Funding:** This research was funded by China National Fund for Distinguished Young Scientists, grant number 51825901; joint fund of the National Natural Science Foundation of China, grant number U20A20318; the Heilongjiang Provincial Science Fund for Distinguished Young Scholars, grant number YQ2020E002; the “Young Talents” Project of Northeast Agricultural University, grant number 18QC28; and a China Postdoctoral Science Foundation Grant [2019M651247].

**Institutional Review Board Statement:** Not applicable.

**Informed Consent Statement:** Not applicable.

**Data Availability Statement:** Data is contained within the article.

**Acknowledgments:** Thanks to the hard-working editors and valuable comments from reviewers.

**Conflicts of Interest:** The authors declare no conflict of interest.

## References

- Hu, G.; Wu, Y.; Liu, B.; Zhang, Y.; You, Z.; Yu, Z. The characteristics of gully erosion over rolling hilly black soil areas of Northeast China. *J. Geogr. Sci.* **2009**, *19*, 309–320. [[CrossRef](#)]
- Mullan, D. Soil erosion under the impacts of future climate change: Assessing the statistical significance of future changes and the potential on-site and off-site problems. *Catena* **2013**, *109*, 234–246. [[CrossRef](#)]
- Chen, H.; Shao, M.; Li, Y. Soil desiccation in the Loess Plateau of China. *Geoderma* **2008**, *143*, 91–100. [[CrossRef](#)]
- Zhao, Y.; Wang, E.; Cruse, R.M.; Chen, X. Characterization of seasonal freeze-thaw and potential impacts on soil erosion in northeast China. *Can. J. Soil Sci.* **2012**, *92*, 567–571. [[CrossRef](#)]
- Cerdà, A.; Keesstra, S.D.; Rodrigo-Comino, J.; Novara, A.; Pereira, P.; Brevik, E.C.; Giménez-Morera, A.; Fernández-Raga, M.; Pulido, M.; Di Prima, S.; et al. Runoff initiation, soil detachment and connectivity are enhanced as a consequence of vineyards plantations. *J. Environ. Manag.* **2017**, *202*, 268–275. [[CrossRef](#)] [[PubMed](#)]
- Ollesch, G.; Kistner, I.; Meissner, R.; Lindenschmidt, K.-E. Modelling of snowmelt erosion and sediment yield in a small low-mountain catchment in Germany. *Catena* **2006**, *68*, 161–176. [[CrossRef](#)]
- Su, J.; Van Bochove, E.; Thériault, G.; Novotná, B.; Khaldoune, J.; Denault, J.; Zhou, J.; Nolin, M.; Hu, C.; Bernier, M.; et al. Effects of snowmelt on phosphorus and sediment losses from agricultural watersheds in Eastern Canada. *Agric. Water Manag.* **2011**, *98*, 867–876. [[CrossRef](#)]
- Nunes, J.; Seixas, J.; Keizer, J. Modeling the response of within-storm runoff and erosion dynamics to climate change in two Mediterranean watersheds: A multi-model, multi-scale approach to scenario design and analysis. *Catena* **2013**, *102*, 27–39. [[CrossRef](#)]
- Behzadfar, M.; Sadeghi, S.H.; Khanjani, M.J.; Hazbavi, Z. Effects of rates and time of zeolite application on controlling runoff generation and soil loss from a soil subjected to a freeze-thaw cycle. *Int. Soil Water Conserv. Res.* **2017**, *5*, 95–101. [[CrossRef](#)]
- Sadeghi, S.H.; Raeisi, M.B.; Hazbavi, Z. Influence of freeze-only and freezing-thawing cycles on splash erosion. *Int. Soil Water Conserv. Res.* **2018**, *6*, 275–279. [[CrossRef](#)]
- Liu, J.; Yu, Z.; Wang, G.; Yao, Q.; Sui, Y.; Shi, Y.; Chu, H.; Tang, C.; Franks, A.E.; Jin, J.; et al. Ammonia-oxidizing archaea show more distinct biogeographic distribution patterns than ammonia-oxidizing bacteria across the black soil zone of Northeast China. *Front. Microbiol.* **2018**, *9*, 171. [[CrossRef](#)] [[PubMed](#)]
- The Ministry of Agriculture of the People's Republic of China. *Classification of Type Regions and Fertility of Cultivated Land in China*; NY/T 309; The Ministry of Agriculture of the People's Republic of China: Beijing, China, 1996; pp. 1–3.
- Yao, Q.; Liu, J.; Yu, Z.; Li, Y.; Jin, J.; Liu, X.; Wang, G. Three years of biochar amendment alters soil physiochemical properties and fungal community composition in a black soil of northeast China. *Soil Biol. Biochem.* **2017**, *110*, 56–67. [[CrossRef](#)]
- Liu, B.Y.; Yan, B.X.; Shen, B.; Wang, Z.Q.; Wei, X. Current status and comprehensive control strategies of soil erosion for cultivated land in the Northeastern black soil area of China. *Sci. Soil Water Conserv.* **2008**, *6*, 1–8. [[CrossRef](#)]
- Yu, D.; Shen, B.; Xie, J. Damages caused by soil and water erosion and their controlling approaches in the black earth area in Northeast China. *J. Soil Water Conserv.* **1992**, *12*, 25–34. [[CrossRef](#)]
- Busch, D.; Kammann, C.; Grünhage, L.; Müller, C. Simple biotoxicity tests forevaluation of carbonaceous soil additives: Establishment and reproducibility off four test procedures. *J. Environ. Qual.* **2012**, *41*, 1023–1032. [[CrossRef](#)] [[PubMed](#)]
- Wang, C.; Walter, M.; Parlange, J.-Y. Modeling simple experiments of biochar erosion from soil. *J. Hydrol.* **2013**, *499*, 140–145. [[CrossRef](#)]
- Singh, B.; Singh, B.P.; Cowie, A.L. Characterisation and evaluation of biochars for their application as a soil amendment. *Aust. J. Soil Res.* **2010**, *48*, 516–525. [[CrossRef](#)]
- Singh, R.; Srivastava, P.; Singh, P.; Sharma, A.K.; Singh, H.; Raghubanshi, A.S. Impact of rice-husk ash on the soil biophysical and agronomic parameters of wheat crop under a dry tropical ecosystem. *Ecol. Indic.* **2019**, *105*, 505–515. [[CrossRef](#)]
- Singh, P.; Singh, R.; Borthakur, A.; Madhav, S.; Singh, V.K.; Tiwary, D.; Srivastava, V.C.; Mishra, P. Exploring temple floral refuse for biochar production as a closed loop perspective for environmental management. *Waste Manag.* **2018**, *77*, 78–86. [[CrossRef](#)]
- Singh, R.; Singh, P.; Singh, H.; Raghubanshi, A.S. Impact of sole and combined application of biochar, organic and chemical fertilizers on wheat crop yield and water productivity in a dry tropical agro-ecosystem. *Biochar* **2019**, *1*, 229–235. [[CrossRef](#)]
- Xu, N.Y.; Li, J. Regional distribution characteristics of cotton fiber quality in main cotton production areas in China. *Chin. J. Eco. Agric.* **2016**, *24*, 1547–1554. [[CrossRef](#)]
- Liu, C.; Chen, L.; Ding, D.; Cai, T. From rice straw to magnetically recoverable nitrogen doped biochar: Efficient activation of peroxymonosulfate for the degradation of metolachlor. *Appl. Catal. B Environ.* **2019**, *254*, 312–320. [[CrossRef](#)]
- Butnan, S.; Deenik, J.L.; Toomsan, B.; Antal, M.J.; Vityakon, P. Biochar characteristics and application rates affecting corn growth and properties of soils contrasting in texture and mineralogy. *Geoderma* **2015**, *237*, 105–116. [[CrossRef](#)]
- El-Naggar, A.; Lee, S.S.; Awad, Y.M.; Yang, X.; Ryu, C.; Rizwan, M.; Rinklebe, J.; Tsang, D.C.; Ok, Y.S. Influence of soil properties and feedstocks on biochar potential for carbon mineralization and improvement of infertile soils. *Geoderma* **2018**, *332*, 100–108. [[CrossRef](#)]
- Atkinson, C.J.; Fitzgerald, J.D.; Hipps, N.A. Potential mechanisms for achieving agricultural benefits from biochar application to temperate soils: A review. *Plant Soil* **2010**, *337*, 1–18. [[CrossRef](#)]
- Farrell, M.; Macdonald, L.M.; Baldock, J.A. Biochar differentially affects the cycling and partitioning of low molecular weight carbon in contrasting soils. *Soil Biol. Biochem.* **2015**, *80*, 79–88. [[CrossRef](#)]

28. De La Rosa, J.M.; Paneque, M.; Hilber, I.; Blum, F.; Knicker, H.; Bucheli, T.D. Assessment of polycyclic aromatic hydrocarbons in biochar and biochar-amended agricultural soil from Southern Spain. *J. Soils Sediments* **2016**, *16*, 557–565. [[CrossRef](#)]
29. Ouyang, L.; Wang, F.; Tang, J.; Yu, L.; Zhang, R. Effects of biochar amendment on soil aggregates and hydraulic properties. *J. Soil Sci. Plant Nutr.* **2013**, *13*, 991–1002. [[CrossRef](#)]
30. Huang, Y.; Liu, D.; An, S. Effects of slope aspect on soil nitrogen and microbial properties in the Chinese Loess region. *Catena* **2015**, *125*, 135–145. [[CrossRef](#)]
31. Hazbavi, Z.; Sadeghi, S.H.; Kiani-Harchegani, M. Application of Biochar on temporal variability of runoff volume and coefficient. In Proceedings of the Third WASWAC Conference, Belgrade, Serbia, 22–26 September 2016; Conference Abstracts Books: Belgrade, Serbia, 2016; pp. 186–187.
32. Sadeghi, S.H.; Hazbavi, Z.; Harchegani, M.K. Controllability of runoff and soil loss from small plots treated by vinasse-produced biochar. *Sci. Total Environ.* **2016**, *541*, 483–490. [[CrossRef](#)]
33. Gul, S.; Whalen, J.K.; Thomas, B.W.; Sachdeva, V.; Deng, H. Physico-chemical properties and microbial responses in biochar-amended soils: Mechanisms and future directions. *Agric. Ecosyst. Environ.* **2015**, *206*, 46–59. [[CrossRef](#)]
34. Sika, M.P.; Hardie, A. Effect of pine wood biochar on ammonium nitrate leaching and availability in a South African sandy soil. *Eur. J. Soil Sci.* **2014**, *65*, 113–119. [[CrossRef](#)]
35. Yuan, P.; Wang, J.; Pan, Y.; Shen, B.; Wu, C. Review of biochar for the management of contaminated soil: Preparation, application and prospect. *Sci. Total Environ.* **2019**, *659*, 473–490. [[CrossRef](#)] [[PubMed](#)]
36. Wang, D.; Fonte, S.J.; Parikh, S.J.; Six, J.; Scow, K.M. Biochar additions can enhance soil structure and the physical stabilization of C in aggregates. *Geoderma* **2017**, *303*, 110–117. [[CrossRef](#)] [[PubMed](#)]
37. Shang, J.; Geng, Z.C.; Chen, X.X.; Zhao, J.; Geng, R.; Wang, S. Effects of biochar on soil organic carbon and nitrogen and their fractions in a rainfed farmland. *J. Environ. Sci. (China)* **2015**, *34*, 509–517.
38. Liu, X.; Mao, P.; Li, L.; Ma, J. Impact of biochar application on yield-scaled greenhouse gas intensity: A meta-analysis. *Sci. Total Environ.* **2019**, *656*, 969–976. [[CrossRef](#)] [[PubMed](#)]
39. Wei, Y.X.; Zhang, Y.P.; Zhang, Y.F.; Wang, R.Y.; Ma, Y.Y.; Zhang, Y. Influences of two consecutive years supply of biochar on soil improvement, water saving and yield increasing in sloping farmland of black soil region. *Trans. CSAM* **2018**, *284*, 291–312.
40. Dong, X.; Li, G.; Lin, Q.; Zhao, X. Quantity and quality changes of biochar aged for 5 years in soil under field conditions. *Catena* **2017**, *159*, 136–143. [[CrossRef](#)]
41. Kettunen, R.; Saarnio, S. Biochar can restrict N<sub>2</sub>O emissions and the risk of nitrogen leaching from an agricultural soil during the freeze-thaw period. *Agric. Food Sci.* **2015**, *22*, 373–379. [[CrossRef](#)]
42. Zhou, Y.; Berruti, F.; Greenhalf, C.; Henry, H.A. Combined effects of biochar amendment, leguminous cover crop addition and snow removal on nitrogen leaching losses and nitrogen retention over winter and subsequent yield of a test crop (*Eruca sativa* L.). *Soil Biol. Biochem.* **2017**, *114*, 220–228. [[CrossRef](#)]
43. Lee, C.-H.; Wang, C.-C.; Lin, H.-H.; Lee, S.S.; Tsang, D.C.; Jien, S.-H.; Ok, Y.S. In-situ biochar application conserves nutrients while simultaneously mitigating runoff and erosion of an Fe-oxide-enriched tropical soil. *Sci. Total Environ.* **2018**, *619*, 665–671. [[CrossRef](#)] [[PubMed](#)]
44. Sadeghi, S.H.; Panah, M.H.G.; Younesi, H.; Kheirfam, H. Ameliorating some quality properties of an erosion-prone soil using biochar produced from dairy wastewater sludge. *Catena* **2018**, *171*, 193–198. [[CrossRef](#)]
45. Jien, S.-H.; Wang, C.-S. Effects of biochar on soil properties and erosion potential in a highly weathered soil. *Catena* **2013**, *110*, 225–233. [[CrossRef](#)]
46. Li, Y.; Zhang, F.; Yang, M.; Zhang, J.; Xie, Y. Impacts of biochar application rates and particle sizes on runoff and soil loss in small cultivated loess plots under simulated rainfall. *Sci. Total Environ.* **2019**, *649*, 1403–1413. [[CrossRef](#)] [[PubMed](#)]
47. Peake, L.R.; Reid, B.J.; Tang, X. Quantifying the influence of biochar on the physical and hydrological properties of dissimilar soils. *Geoderma* **2014**, *235*, 182–190. [[CrossRef](#)]
48. Reddy, K.R.; Yaghoubi, P.; Aksoy, Y.Y. Effects of biochar amendment on geotechnical properties of landfill cover soil. *Waste Manag. Res.* **2015**, *33*, 524–532. [[CrossRef](#)]
49. Gao, H.; Shao, M. Effects of temperature changes on soil hydraulic properties. *Soil Tillage Res.* **2015**, *153*, 145–154. [[CrossRef](#)]
50. Ma, Q.; Zhang, K.; Jabro, J.D.; Ren, L.; Liu, H. Freeze–thaw cycles effects on soil physical properties under different degraded conditions in Northeast China. *Environ. Earth Sci.* **2019**, *78*, 321. [[CrossRef](#)]
51. Hou, R.; Li, T.; Fu, Q.; Liu, D.; Cui, S.; Zhou, Z.; Yan, P.; Yan, J. Effect of snow-straw collocation on the complexity of soil water and heat variation in the Songnen Plain, China. *Catena* **2019**, *172*, 190–202. [[CrossRef](#)]
52. Wu, Y.; Ouyang, W.; Hao, Z.; Lin, C.; Liu, H.; Wang, Y. Assessment of soil erosion characteristics in response to temperature and precipitation in a freeze-thaw watershed. *Geoderma* **2018**, *328*, 56–65. [[CrossRef](#)]
53. Fang, H.-J.; Yang, X.; Zhang, X.-P.; Liang, A. Using 137 CS tracer technique to evaluate erosion and deposition of black soil in northeast china. *Pedosphere* **2006**, *16*, 201–209. [[CrossRef](#)]
54. Yu, Z.-H.; Yu, J.; Ikenaga, M.; Sakai, M.; Liu, X.-B.; Wang, G.-H. Characterization of root-associated bacterial community structures in soybean and corn using locked nucleic acid (LNA) oligonucleotide-PCR clamping and 454 pyrosequencing. *J. Integr. Agric.* **2016**, *15*, 1883–1891. [[CrossRef](#)]
55. Fu, Q.; Hou, R.; Li, T.; Wang, M.; Yan, J. The functions of soil water and heat transfer to the environment and associated response mechanisms under different snow cover conditions. *Geoderma* **2018**, *325*, 9–17. [[CrossRef](#)]

56. Tian, D.; Qu, Z.Y.; Gou, M.M.; Li, B.; Lv, Y.J. Experimental study of influence of biochar on different texture soil hydraulic characteristic parameters and moisture holding properties. *Pol. J. Environ.* **2015**, *24*, 1435–1442.
57. O'Kelly, B.C. Accurate determination of moisture content of organic soils using the oven drying method. *Dry. Technol.* **2004**, *22*, 1767–1776. [[CrossRef](#)]
58. Shen, H.; Zheng, F.; Wen, L.; Han, Y.; Hu, W. Impacts of rainfall intensity and slope gradient on rill erosion processes at loessial hillslope. *Soil Tillage Res.* **2016**, *155*, 429–436. [[CrossRef](#)]
59. Liu, G.; Hu, F.; Zheng, F.; Zhang, Q. Effects and mechanisms of erosion control techniques on stairstep cut-slopes. *Sci. Total Environ.* **2019**, *656*, 307–315. [[CrossRef](#)]
60. Lv, J.; Luo, H.; Xie, Y.-S. Effects of rock fragment content, size and cover on soil erosion dynamics of spoil heaps through multiple rainfall events. *Catena* **2019**, *172*, 179–189. [[CrossRef](#)]
61. Gholami, L.; Sadeghi, S.H.; Homaei, M. Straw mulching effect on splash erosion, runoff, and sediment yield from eroded plots. *Soil Sci. Soc. Am. J.* **2013**, *77*, 268–278. [[CrossRef](#)]
62. Li, Z.B.; Li, S.X.; Ren, Z.P.; Li, P.; Wang, T. Effects of freezing-thawing on hillslope erosion process. *J. Soil Water Conserv.* **2015**, *29*, 56–60. [[CrossRef](#)]
63. Ye, Z.Y. On the Selection of Index Forward and Dimensionless Methods in Multi-index Comprehensive Evaluation. *J. Stat. Theory Pract.* **2003**, *4*, 24–25. [[CrossRef](#)]
64. Liu, Y.; Wang, X.; Zhou, L.; Zan, X.; Sheng, S. Relationship analysis between soil detachment rate and erosion factors on freeze-thaw slope. *Trans. CSAE* **2016**, *32*, 136–141. [[CrossRef](#)]
65. Fu, Q.; Zhao, H.; Li, T.; Hou, R.; Liu, D.; Ji, Y.; Zhou, Z.; Yang, L. Effects of biochar addition on soil hydraulic properties before and after freezing-thawing. *Catena* **2019**, *176*, 112–124. [[CrossRef](#)]
66. Li, Z.-G.; Gu, C.; Zhang, R.; Ibrahim, M.; Zhang, G.-S.; Wang, L.; Chen, F.; Liu, Y. The benefic effect induced by biochar on soil erosion and nutrient loss of slopping land under natural rainfall conditions in central China. *Agric. Water Manag.* **2017**, *185*, 145–150. [[CrossRef](#)]
67. Juan, Y.; Tian, L.; Sun, W.; Qiu, W.; Curtin, D.; Gong, L.; Liu, Y. Simulation of soil freezing-thawing cycles under typical winter conditions: Implications for nitrogen mineralization. *J. Soils Sediments* **2019**, *20*, 143–152. [[CrossRef](#)]
68. Brodowski, S.; John, B.; Flessa, H.; Amelung, W. Aggregate-occluded black carbon in soil. *Eur. J. Soil Sci.* **2006**, *57*, 539–546. [[CrossRef](#)]
69. Sachdeva, V.; Hussain, N.; Husk, B.R.; Whalen, J.K. Biochar-induced soil stability influences phosphorus retention in a temperate agricultural soil. *Geoderma* **2019**, *351*, 71–75. [[CrossRef](#)]
70. Wang, G.; Jin, J.; Chen, X.; Liu, J.; Liu, X.; Herbert, S. Biomass and catabolic diversity of microbial communities with long-term restoration, bare fallow and cropping history in Chinese Mollisols. *Plant Soil Environ.* **2008**, *53*, 177–185. [[CrossRef](#)]
71. He, X.; Yin, H.; Sun, X.; Han, L.; Huang, G. Effect of different particle-size biochar on methane emissions during pig manure/wheat straw aerobic composting: Insights into pore characterization and microbial mechanisms. *Bioresour. Technol.* **2018**, *268*, 633–637. [[CrossRef](#)]
72. Liu, Z.; Dugan, B.; Masiello, C.A.; Barnes, R.T.; Gallagher, M.E.; Gonnermann, H. Impacts of biochar concentration and particle size on hydraulic conductivity and DOC leaching of biochar–sand mixtures. *J. Hydrol.* **2016**, *533*, 461–472. [[CrossRef](#)]
73. Lee, S.S.; Shah, H.S.; Awad, Y.M.; Kumar, S.; Ok, Y.S. Synergy effects of biochar and polyacrylamide on plants growth and soil erosion control. *Environ. Earth Sci.* **2015**, *74*, 2463–2473. [[CrossRef](#)]
74. Smetanová, A.; Dotterweich, M.; Diehl, D.; Ulrich, U.; Dotterweich, N.F. Influence of biochar and terra preta substrates on wettability and erodibility of soils. *Z. Geomorphol.* **2013**, *57*, 111–134. [[CrossRef](#)]
75. Le Bissonnais, Y.; Arrouays, D. Aggregate stability and assessment of soil crustability and erodibility: II. Application to humic loamy soils with various organic carbon contents. *Eur. J. Soil Sci.* **1997**, *48*, 39–48. [[CrossRef](#)]
76. Peng, X.; Zhu, Q.H.; Xie, Z.; Darboux, F.; Holden, N.M. The impact of manure, straw and biochar amendments on aggregation and erosion in a hillslope Ultisol. *Catena* **2016**, *138*, 30–37. [[CrossRef](#)]
77. Abrol, V.; Ben-Hur, M.; Verheijen, F.G.A.; Keizer, J.J.; Martins, M.A.S.; Tenaw, H.; Tchekansky, L.; Graber, E.R. Biochar effects on soil water infiltration and erosion under seal formation conditions: Rainfall simulation experiment. *J. Soils Sediments* **2016**, *16*, 2709–2719. [[CrossRef](#)]
78. Lee, S.S.; Gantzer, C.J.; Thompson, A.L.; Anderson, S.H.; Ketcham, R.A. Using High-Resolution Computed Tomography Analysis to Characterize Soil-Surface Seals. *Soil Sci. Soc. Am. J.* **2008**, *72*, 1478–1485. [[CrossRef](#)]
79. Doan, T.T.; Henry-Des-Tureaux, T.; Rumpel, C.; Janeau, J.-L.; Jouquet, P. Impact of compost, vermicompost and biochar on soil fertility, maize yield and soil erosion in Northern Vietnam: A three year mesocosm experiment. *Sci. Total Environ.* **2015**, *514*, 147–154. [[CrossRef](#)]
80. Wei, Y.X.; Shi, G.X.; Wu, Y.; Liu, H. Effect and comprehensive evaluation of biochar application mode on slope farmland in black soil region. *Chin. Soc. Agric. Mach.* **2018**, *49*, 251–259. [[CrossRef](#)]